ACS MATERIALS LETTERS

www.acsmaterialsletters.org

LETTER

Gelatin-Coated Copper-Based Metal–Organic Framework for Controlled Insulin Delivery: Possibility toward Oral Delivery System

Pawan Kumar, Navpreet Kaur, Pranav Tiwari, Anoop Kumar Gupta, and Shaikh M. Mobin*

Cite This: *ACS Materials Lett.* 2023, 5, 1100–1108

Read Online

ACCESS | Metrics & More | Article Recommendations | Supporting Information

ABSTRACT: **The development of nontoxic, hemocompatible materials for controlled insulin delivery is a great challenging task for researchers. Herein, we demonstrate the design of a novel linker 5,5′-((pyridine-2,6-diylbis(methylene)) bis(oxy))-diisophthalic acid (H_4L) and its utilization to synthesize a new Cu-MOF (IITI-3). IITI-3 crystallizes in a tetragonal crystal system with space group *I*4/*mmm* and shows a high Brunauer–Emmett–Teller (BET) surface area of 1026.5 m^2/g with pore diameter (Barrett–Joyner–Halenda pore size distribution) of 3.413 nm. The IITI-3 is found to be stable in the biological fluid pH ranges from 3 to 10. Moreover, IITI-3 were explored for insulin delivery by coating the IITI-3 with gelatin (gel@insIITI-3); the overall insulin was controlled from the framework. The obtained result paves a new avenue for the oral delivery of insulin using the IITI-3 metal-organic framework.**

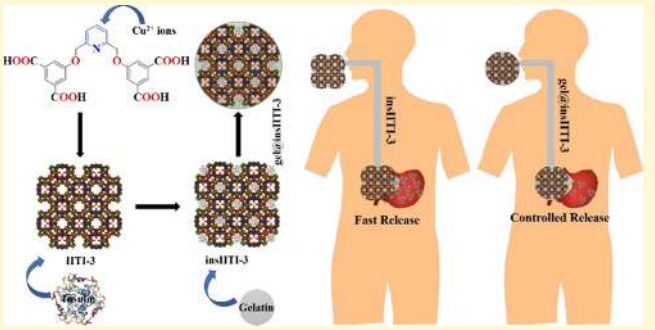

INTRODUCTION

Diabetes miletus (DM) is the most challenging disease[1] and mainly occurs in two types: type I (T1DM) and type II (T2DM). In T1DM, the body does not produce enough insulin, and contrarily T1DM is also known as insulin resistance in which either the body fails to produce insulin or shows resistance toward insulin.[2] Beta cells are responsible for the production of insulin in the body. In T1DM, the autoimmune system kills the beta cells resulting in less or no production of insulin.[3] Hyperglycemia occurs when there is an excess of glucose in the blood and the body does not produce or use enough insulin in the case of T2DM.[4] T2DM significantly increases the risk of both macrovascular alterations and microvascular consequences, such as retinopathy, neuropathy, and nephropathy.[5−8] Different medicines have been developed to treat T1DM and T2DM, but direct insulin injection continues to be the only therapeutic option that is currently effective for patients.[9] Good glycemic control in T1DM typically necessitates at least two (and frequently three or more) daily insulin injections.[10,11] Therefore, the development of oral insulin delivery systems is required to lessen the discomfort and pain experienced by patients who frequently consume insulin subcutaneously via injection. The subcutaneously injected insulin may cause peripheral hyperinsulinemia and related problems, but when administered orally is more capable of passing through the liver similarly to physiologically produced insulin.[12] However, oral medication distribution has severe complications, including issues with stability in the gastrointestinal (GI) tract, solubility, bioavailability, and dissolution. Several oral insulin formulations have undergone clinical testing; however, substantial commercial development has not yet been accomplished.[13]

The proposed system must include a biocompatible, high-loading platform that protects insulin from external acidic environments and enzymatic degradation, as well as targeted drug delivery coupled with stimuli-responsive drug release, such as hyperglycemia, in order to be considered an efficient oral insulin delivery method.[14] Currently, various materials are employed for oral delivery (such as liposomes, nanoemulsions, nanoparticles, or micelles)[15−18] but they are largely ineffective; improved methods are therefore required to solve the drawbacks. Recently, the metal–organic-frameworks (MOFs) have established themselves as an exciting candidate for different biomedical applications such as drug delivery, bioimaging and sensing etc. because of their tunable size,

Received: December 13, 2022
Accepted: March 8, 2023
Published: March 10, 2023

https://doi.org/10.1021/acsmaterialslett.2c01175
ACS Materials Lett. 2023, 5, 1100–1108

Scheme 1. Schematic Synthesis of H_4L

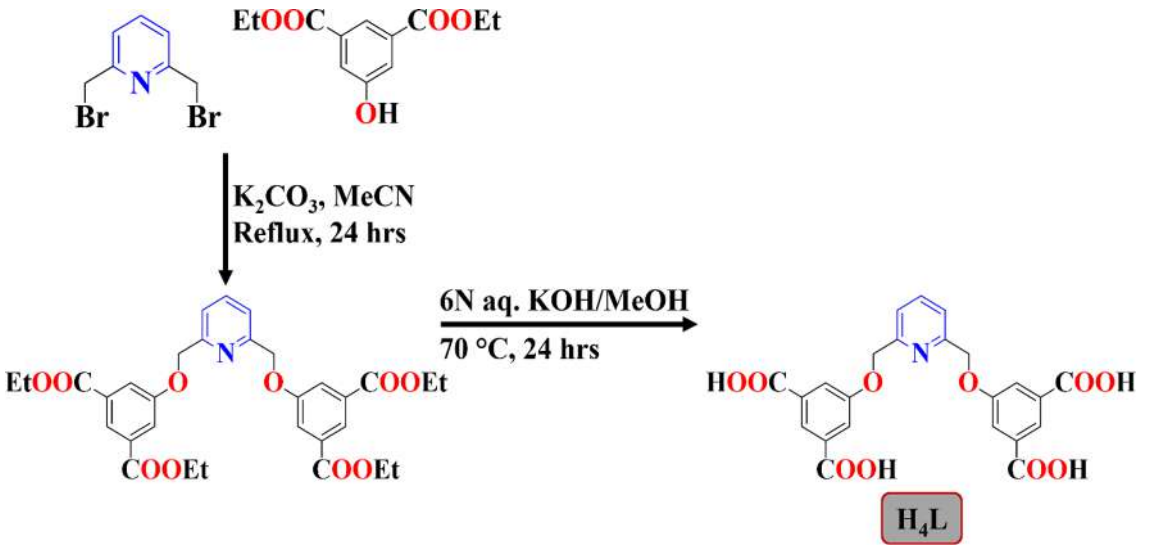

Scheme 2. Schematic Synthesis of IITI-3

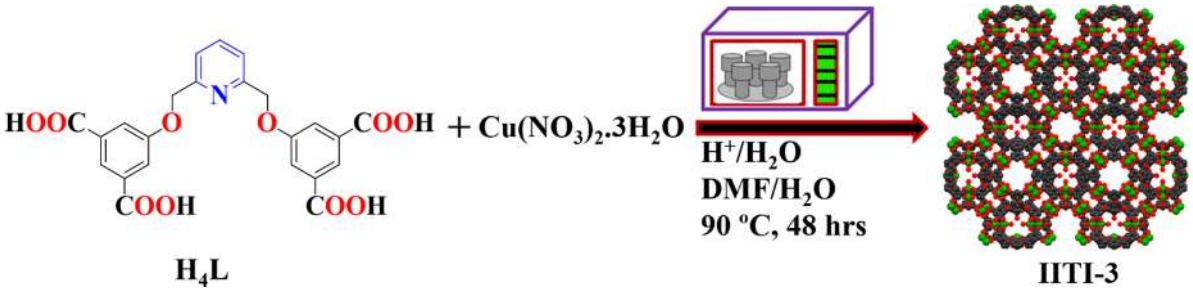

high porosity, and range of starting materials.[19−22] Among different biomedical applications of MOF, its suitability toward drug delivery can be more diverse and impactful because it can encapsulate different therapeutic molecules in their cavities with high loading and then can deliver drugs in a controlled manner; because of the release of the drug molecule from the framework, it takes more time, because of the breaking of interactions between framework and drug molecules, which usually cannot be possible with different other nano/biomaterials. MOFs themselves are well-known for controlled drug release, because drug are stored within the pores, on the surface of the framework, and upheld by the electrostatic interaction (hydrophilic or hydrophobic), hydrogen bonding, van der Waals, the $\pi-\pi$ interaction, coordination bonds, and anion−cation electrostatic interaction.[23,24] Generally, the Co-, Ni-, and Cr-based MOFs revealed in these studies were incompatible with biological and pharmacological applications, due to the toxic nature of metal present within the framework. However, in the case of ionic drugs, the strong electrostatic interaction between ionic drugs and ionic frameworks plays a crucial role.[25] Large surface area and high porosity (mesoporous and macroporous) of MOFs is necessary condition for high drug loading, large protein molecules encapsulation. Cu-MOFs, Fe-MOFs, and Zn-MOFs are highly biocompatible, hemocompatible, and biodegradable in nature. But most of the MOFs degrades in a wide range of pH (3−10), and also are not stable in the medium. Apart from that most of the framework is losing their identity after gelatin coating. Upon comparing MOFs with chitosan-based nanocomposites, they have less surface area, are unstable at alkaline pH, and do not have tunable pore size; however, in the case of MOFs, they have high surface area and are stable over a wide range of pH, from acidic to alkaline.[26,27] Additionally, MOFs can keep proteins active in hostile environments like stomach fluid (pH 1.5−3.5), simulated physiological conditions (pH 7.2−7.4), and organic solvents.[28−30]

Currently, the sustainable release of drugs from MOFs have gained considerable interest.[31] However, three primary approaches have been employed up to this point: (i) coating-controlled drug release; (ii) drug release regulated by drug-matrix interaction, and (iii) drug release initiated by cations.[32,33] In the coating-controlled drug release method, majorly synthetic or natural polymeric materials are used to create microparticulate delivery systems. Gelatin is one of the natural polymers, which is used extensively in the pharmaceutical industry, because of its outstanding biocompatible nature, excellent degradability to nontoxic chemicals, and low cost.[34,35] Gelatin also increases the biocompatibility of materials. In 2019, Nezhad-Mokhtari et al.[36] performed methotrexate delivery via gelatin-coated Cu-MOF in a very sustainable manner. Similarly, in 2019, Javanbakht et al.[37] performed ibuprofen oral delivery via gelatin-coated Cu-MOF in a controlled manner.

Herein, we have designed/synthesized a new three-dimensional (3D) Cu-MOF named **IITI-3** utilized for drug encapsulation by insulin and Hum-insulin (insulin that is commercially available). After encapsulation with insulin, termed as **insIITI-3**, and further coated with gelatin formed

https://doi.org/10.1021/acsmaterialslett.2c01175
ACS Materials Lett. 2023, 5, 1100−1108

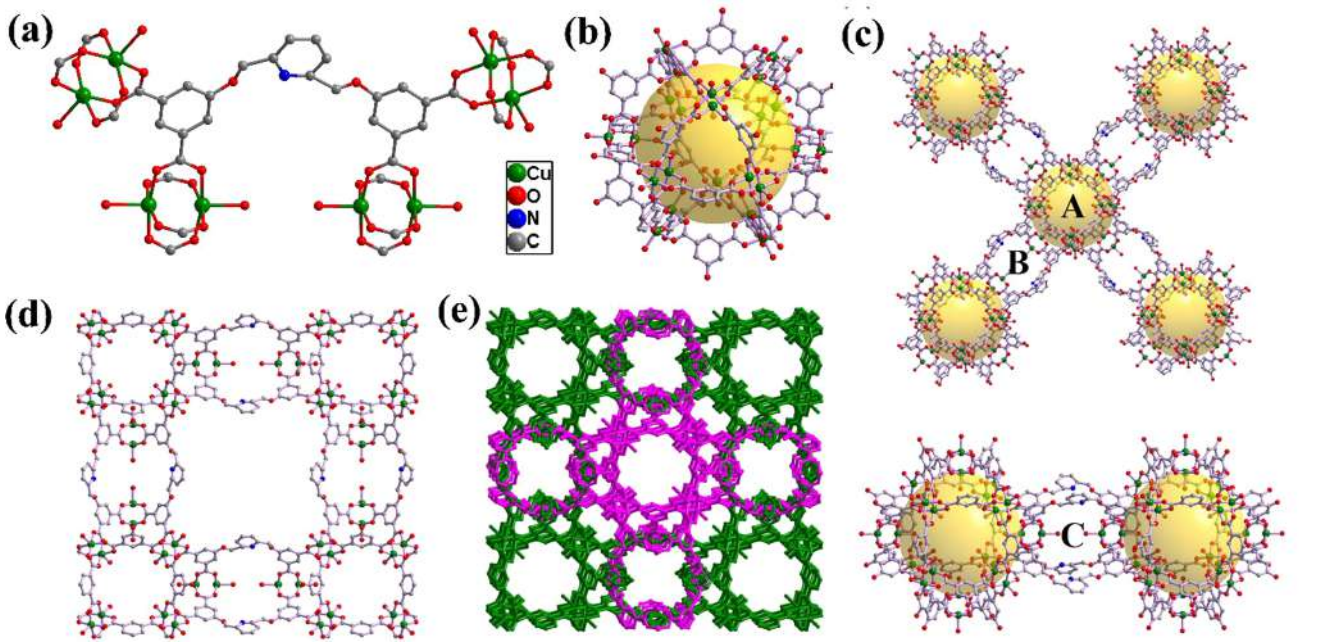

Figure 1. (a) H_4L ligation with Cu^{2+} ions to form IITI-3 containing $[Cu_2(COO)_4]$ SBUs, (b) interconnection of 12 such SBUs produces a typical metal−organic cuboctahedron (MOC, cavity A), (c) interconnection of MOCs in the *ab*-plane and *c*-axis by H_4L units. (d) Illustration of the 3D framework along the *c*-axis, and (e) 2-fold interpenetrated 3D frameworks.

as **gel@insIITI-3** to explore its release pattern in different pH conditions toward their control release.

A novel tetracarboxylic acid linker H_4L was synthesized by the substitution reaction of 2,6-(bisbromomethyl)pyridine, and 5-hydroxyisophthalate in the presence of K_2CO_3 in acetonitrile solvent, followed by basic hydrolysis resulting in the formation of H_4L, which is well-characterized by high-resoultion mass spectrometry (HRMS) and nuclear magnetic resonance (NMR) spectroscopy [Scheme 1; the detailed synthetic procedure is given in the Supporting Information (SI) (Figures S1−S6)].

The solvothermal reaction of the novel tetracarboxylic acid linker (H_4L) and $Cu(NO_3)_2{\cdot}3H_2O$ in a mixed solvent system (DMF + H_2O) under a Teflon-lined autoclave resulted in a blue-colored block-shaped single crystals of **IITI-3** (Scheme 2; the detailed synthetic procedure is given in the SI).

The single-crystal X-ray diffraction (SCXRD) studies of **IITI-3** reveal that it crystallizes in the tetragonal *I*4/*mmm* space group (Table S1 in the SI). In the framework of **IITI-3**, both isophthalate units of the H_4L linker utilizes four carboxylate groups to link eight Cu(II) ions which are further extended through the coordination of carboxylate groups from the other H_4L linkers. All the Cu(II) ions are equatorially coordinated by carboxylate's oxygens from the different H_4L linkers [Cu−O: 1.944(4)−1.962(6) Å] and axially occupied by water molecules [Cu−O: 2.094(10)−2.147(8) Å (Table S2 in the SI), leading to a square pyramidal geometry.

The combination of two such square pyramidal Cu(II) centers forms a typical inorganic paddlewheel (PW) $[Cu_2(COO)_4{\cdot}2H_2O]$ as secondary building units (SBUs) with the Cu−Cu separation of 2.6477(14)−2.6549(18) Å (Table S2) (Figure 1a). Again, such units are extended through Cu(II)−OOC linkage to generate a highly porous framework called metal−organic cuboctahedron (MOC) that contains three types of microporous cavities: A, B, and C (Figures 1b and 1c). A closer view of the framework shows that the isophthalate moiety of H_4L connects to two Cu_2 PW-SBUs; again, 12 such PW-SBUs were spanned by 24 isophthalate units from different H_4L linkers to produce edge-directed corner-linked MOCs containing cavity A (15.86 Å) (Figure 1c). The MOC consists of eight and six triangular and square windows, respectively, which will allow guest molecules to enter the interior cavities. The vicinal MOCs are further interconnected through the H_4L spacer producing two more types of cavities B and C (7.84 Å). The linking of two PW-SBUs by four H_4L units produces cavity B, and the linking of two clusters of four SBUs by four H_4L units produces cavity C. Furthermore, each MOC was interconnected with six neighboring MOCs through 24 H_4L moieties, resulting in four and two cavities of types B and C, respectively, surrounding each MOC. Additionally, **IITI-3** exhibits 2-fold interpenetration and generates a fourth pseudo-cavity that is filled with a MOC from the second framework (Figures 1d and 1e). However, the channels formed via the open windows of the MOC nodes and the C cavities persist along the *c*-axis. The channels were filled by disordered lattices solvent molecules, which were treated by SQUEEZE refinement of PLATON to calculate the effective solvent-accessible void volume and found to be 48.7% ($Å^3$) per unit cell. The highly porous nature and larger cavities of **IITI-3** offer appropriate corridors for insulin loading and acting as a suitable cargo for insulin delivery.

The single-crystal structural studies reveals that the **IITI-3** has the larger cavity, i.e., cavity A ∼16 Å in size. The particle size of monomeric insulin is 13 Å,[38] and, at pH 7.4, insulin forms tetramers 25 ± 3 Å in size.[39] Therefore, it could be possible that the monomeric insulin can fit in cavity A, and allowed insulin to diffuse through the framework and to be released from the MOF's cavities/pores.

Furthermore, we have used gelatin as coating material, because of its extensive use in the food, beauty, pharmaceutical industries, easy availability, and excellent structural stabil-

https://doi.org/10.1021/acsmaterialslett.2c01175
ACS Materials Lett. 2023, 5, 1100−1108

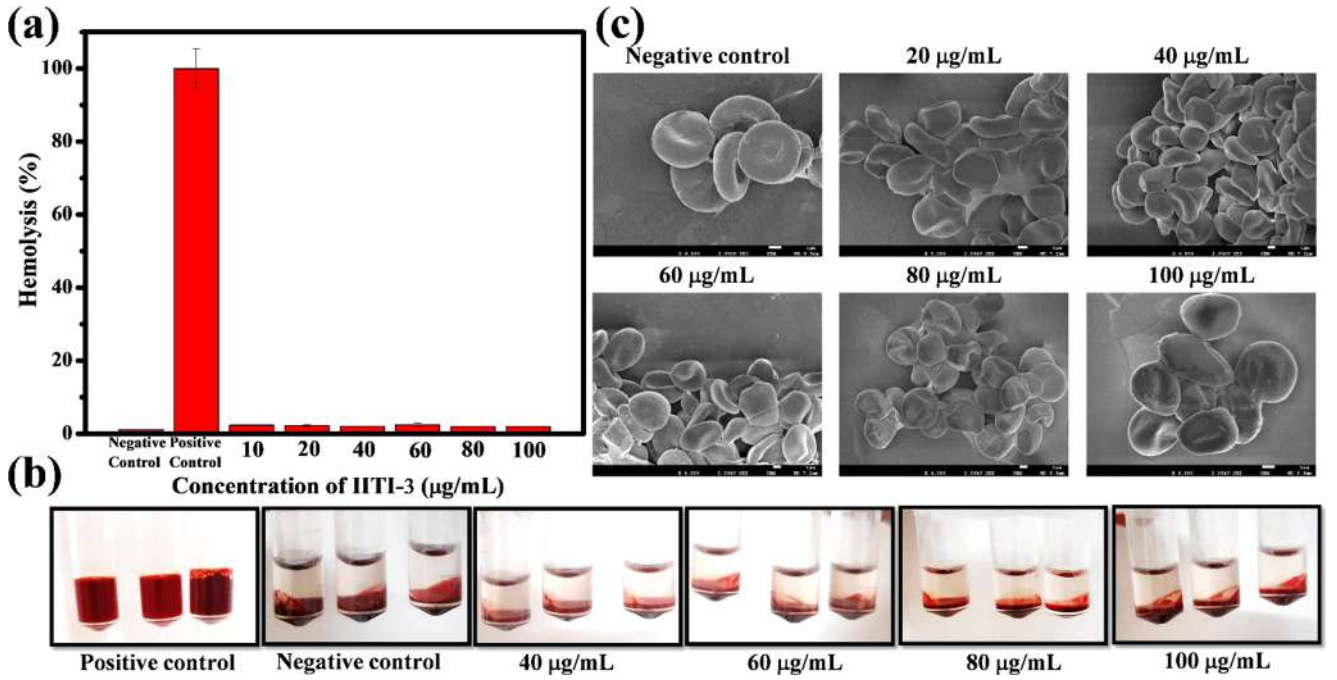

Figure 2. Hemocompatibility of IITI-3. (a) The percentage hemolysis graph after incubating RBCs with different concentrations of IITI-3 for 1 h, (b) the images of the centrifuged samples (control and treated), and (c) the SEM images of negative control and IITI-3-treated RBCs.

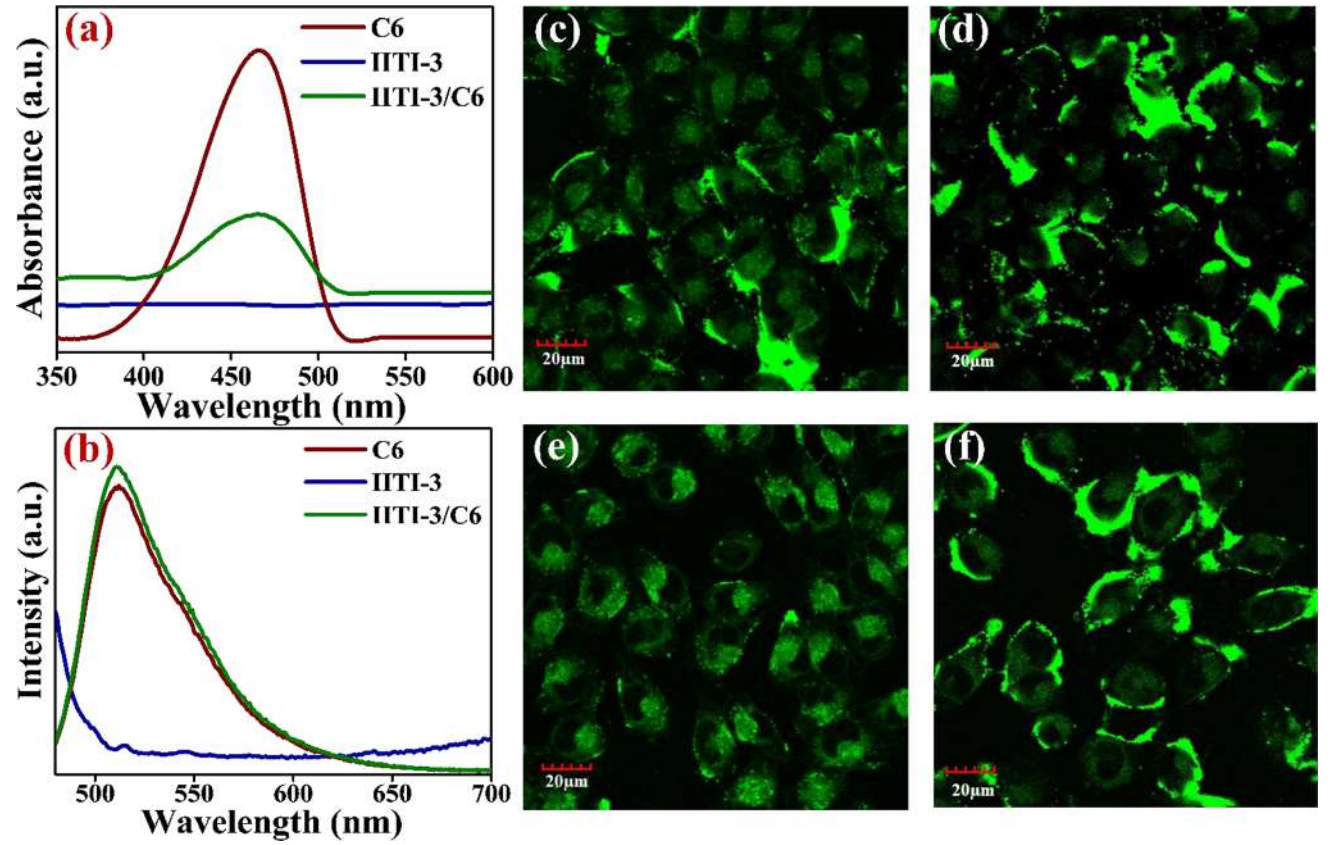

Figure 3. (a) UV-vis spectra of C6, IITI-3, and IITI-3/C6; (b) emission spectra of C6, IITI-3, and IITI-3/C6. In vitro cellular uptake assay: fluorescence ($\lambda_{ex}/\lambda_{em}$ = 488/520 ± 25 nm) images of cells treated with (c) IITI-3/C6, (d) insIITI-3/C6, (e) gel@IITI-3/C6, and (f) gel@insIITI-3/C6.

ity.[40,41] Prior of applying **IITI-3** for insulin delivery, its cellular and hemocompatibility studies were performed and detailed explanation were provided in the SI (see Figures S7 and S8a). The effect of **IITI-3** on the red blood cells (RBCs) was

https://doi.org/10.1021/acsmaterialslett.2c01175
ACS Materials Lett. 2023, 5, 1100−1108

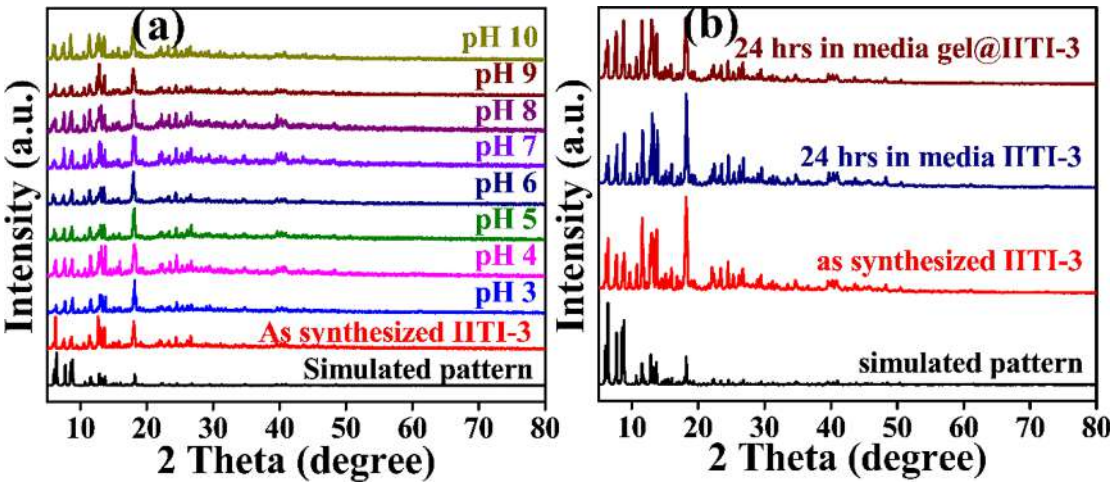

Figure 4. PXRD of IITI-3 (a) simulated, as synthesized, at different pH values from pH 3 to pH 10, and (b) simulated, as-synthesized, IITI-3 and gel@IITI-3 in media after treatment for 24 h.

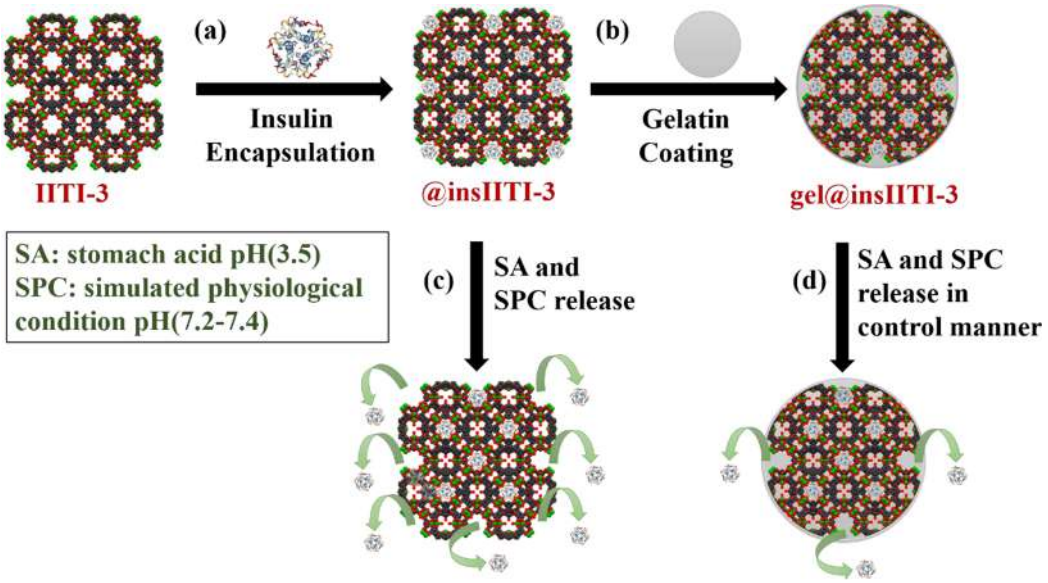

Figure 5. (a) Insulin encapsulation IITI-3 and the (b) gelatin coating on insIITI-3; panels (c) and (d) show insulin release profiles from insIITI-3 and gel@insIITI-3 in stomach acid and SPC pH, respectively.

checked through hemolysis assay. The result shown in Figure 2a clearly indicate the hemocompatible nature of **IITI-3**. Even the high concentration of **IITI-3** showed very less hemolysis, i.e., <3%. The positive control clearly shows the red color of the supernatant generated by the presence of free hemoglobin, but the treated samples with **IITI-3** lack any red supernatant color and resemble the color of the negative control (Figure 2b). Hemocompatible materials are those that exhibit <5% hemolysis. The biconcave shape of RBCs is further confirmed by the SEM images of RBCs treated with different concentrations of **IITI-3**, which further support the hemocompatible nature of **IITI-3** and surface passivation therefore supports its nonhemolytic character (Figure 2c).[42] The internalization of **IITI-3**, **gel@IITI-3**, **insIITI-3**, and **gel@insIITI-3** in MCF-7 cells was checked for its effective cellular uptake by conjugating the framework with fluorescent dye C6 (Coumarin 6). As shown in Figure 3, the clear green fluorescence (bright-field images given in Figure S8b in the SI) arising from the cytoplasm of the treated cells shows the effective uptake of **IITI-3**, **gel@IITI-3**, **insIITI-3**, and **gel@insIITI-3**. The C6 dye **IITI-3** conjugation was confirmed using ultraviolet−visible light (UV-vis) spectroscopy and fluorescence spectroscopy. The new UV peak at ∼470 nm of **IITI-3/C6** coincide with the peak of C6. Similarly, in fluorescence spectroscopy, **IITI-3/C6** exhibits a peak at 510 nm, which was coincide with C6 dye.

Apart from that, the structural stability of **IITI-3** was also checked by powder X-ray diffraction (PXRD) (Figure 4a) and SEM images (Figure S9 in the SI) under different pH conditions (pH 3−10) to mimic simulated gastric fluid condition pH (pH 1.5−3.5) and simulated physiological condition (SPC) pH (7.2−7.4). The obtained result supported the "stability of **IITI-3** at various physiological conditions" and motivated us to use them for insulin delivery. Furthermore, the stability of **IITI-3** and gelatin coated **gel@IITI-3** were checked in Dulbecco's Modified Eagle Medium (DMEM) containing 10% fetal bovine serum (FBS). The **IITI-3** and gelatin coated **gel@IITI-3** were stable, even in the cell culture media, as shown in PXRD (Figure 4b).

https://doi.org/10.1021/acsmaterialslett.2c01175
ACS Materials Lett. 2023, 5, 1100−1108

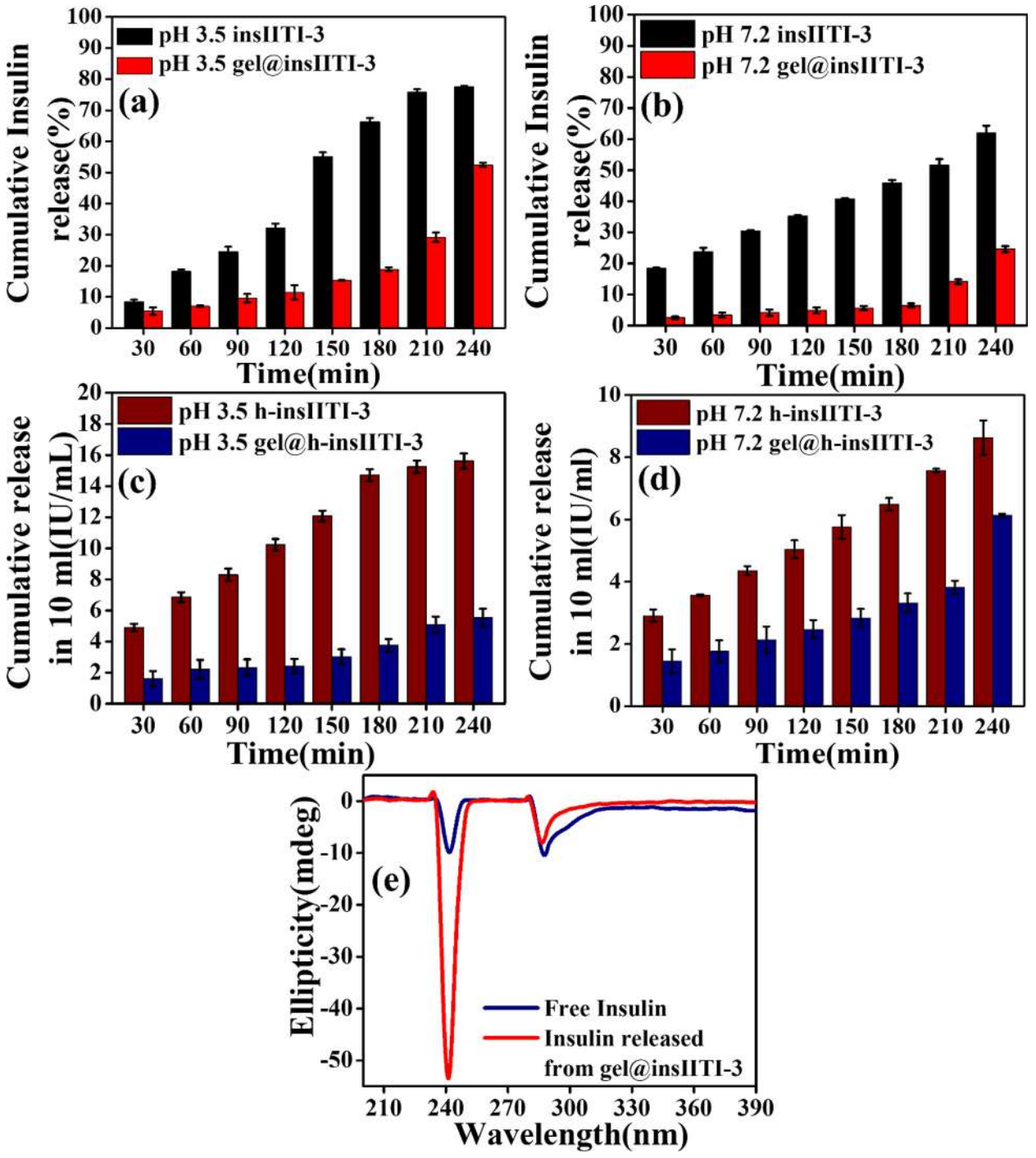

Figure 6. Cumulative insulin release from (a) insIITI-3 and gel@insIITI-3 at pH 3.5, (b) insIITI-3 and gel@insIITI-3 at pH 7.2, (c) h-insIITI-3 and gel@h-insIITI-3 at pH 3.5, (d) h-insIITI-3 and gel@h-insIITI-3 at pH 7, and (e) CD spectra of free insulin and insulin released from gel@insIITI-3.

IITI-3 showed all the effective attributes needed for an oral delivery nanocarrier. Because of good biocompatibility (stable in wide pH range (pH 3−10) and cell media) favors **IITI-3** as a potential candidate as a drug delivery carrier with insulin. Also, by modifying the nanocarrier with high surface area (1056.5 m^2/g), pore diameter (3.413 nm), (see Figures S10, S14d, and S14e in the SI), hemocompatibility with proteins/biomolecules offers advantages like "modulation of the immune response, variation of in vivo biodistribution and generation of stealth property", which ultimately may improve the delivery pattern.[43] Recently, Tian and co- workers[44] reported decorating UiO-68-NH_2 with transferrin for controlled insulin delivery. For the drug delivery phenomenon, the **IITI-3** was encapsulated with insulin and for control release, it was further modified with gelatin. The schematic representation for the formation of **ins@IITI-3** and **gel@insIITI-3** is shown in Figures 5a and 5b. The **IITI-3** was activated, further modified as **insIITI-3** and **gel@insIITI-3**, which were characterized by PXRD, TGA, FT-IR, BET adsorption isotherm, and SEM (EDX). Their analysis is thoroughly

https://doi.org/10.1021/acsmaterialslett.2c01175
ACS Materials Lett. 2023, 5, 1100−1108

explained in the SI (see Figures S10−S17). The drug loading content (DLC) after insulin encapsulation (**insIITI-3**) was determined to be 20 wt % and also found to be in commercially available insulin (Hum-insulin). The DLC is calculated by measuring the absorbance of supernatant after loading via UV-vis spectroscopy and with the help of a linearity plot (see Figures S12 and S13 in the SI) by employing the DLC formula (eq S1 in the SI). Furthermore, DLS showed an increase in hydrodynamic diameter after gelatin coating in **IITI-3** (**gel@IITI-3**), which confirmed that gelatin is successfully covered throughout the surface of **IITI-3** (see Figure S18 in the Supporting Information). The zeta potential values of **IITI-3** and **gel@insIITI-3** are −20.8 mV and −12.40 mV, respectively (see Figure S19 in the Supporting Information).

Drug loading was confirmed by the increase in the weight percentage in TGA. From BET surface area and BJH pore size distribution, it has been confirmed that the pore size decreases from 3.412 nm to 3.406 nm and the surface area decreases from 1026.516 m^2/g to 576.11 m^2/g. It has been confirmed that the pore of the **IITI-3** that is filled with insulin decreases in surface area, which suggests that insulin is also present on the surface of the **IITI-3**. The possible reason for the insulin loading within the framework is either hydrophobic and/or electrostatic interaction between **IITI-3** and insulin molecules.[31] Furthermore, gelatin coating has been performed on the **insIITI-3**. A drug release profile has been obtained via a dialysis method. The fast drug release from the **insIITI-3** has been related to the diffusion method.[24,45,46] In this method, insulin comes out from the channel present inside to the **insIITI-3** to the solution. In stomach acid (pH 3.5), drug release is faster in comparison to SPC (pH 7.2); a possible reason is that the solubility of insulin increases as the pH decreases. However, in the case of gelatin-coated **insIITI-3** (**gel@insIITI-3**), drug release is regulated with the gelatin corona which covered the surface of the **insIITI-3**. Therefore, in this work, gelatin provide the barrier for insulin, which is releasing from **insIITI-3.** To examine the release profile of regular insulin (r-insulin) from **insIITI-3** and **gel@insIITI-3**, we have taken the solution of pH 3.5, and pH 7.2 (Figures 5c and 5d). These pH value corresponds to stomach acid (pH 1.5−3.5) and SPC (pH 7.2−7.4). The graphs shown in Figures 6a−d) indicate that both the **insIITI-3** and the **gel@insIITI-3** loaded with insulin have sustained-release characteristics. The developed carriers **insIITI-3** and **gel@insIITI-3** release insulin gradually and over a period of time, up to 4 h.

By comparison with Figures 6a−d, it is evident that the drug release from **IITI-3** could be regulated by using a polymer coating comprised of gelatin material. As the pH value increases, the percentage drug release decreases; this might be connected to the gelatin polymer's pH sensitivity and the gelatin microsphere polymeric network's diffusion barrier. The same pattern was observed in the case of Hum-insulin **h-insIITI-3** and **gel@h-insIITI-3** (Figures 6c and 6d). The gelatin-coated **IITI-3** gives controlled results with respect to time and rate, as compared to the recent reports (see Table S3 in the SI).

Using circular dichroism (CD) spectroscopy, the insulin conformational changes were assessed. As seen in Figure 6e, neither the insulin that was released from **gel@insIITI-3** nor the normal insulin underwent any substantial structural changes, demonstrating that the insulin maintenance was confirmed, even after its release.

CONCLUSION

In conclusion, in the present work, a new **Cu-MOF**, termed as **IITI-3**, were prepared solvo-thermally by utilizing a novel H_4L linker. Moreover, the **IITI-3** showed excellent structural stability, biocompatibility, and hemocompatibility. Also, because of its very high porosity, **IITI-3** had good protein-drug loading (insulin) (up to 20 wt %). Furthermore, coating the **insIITI-3** with gelatin gives more controlled release of insulin, compared to uncoating under physiological conditions. The gelatin coating on **insIITI-3** was done in a facile manner to amend the release pattern of encapsulated insulin, thus providing the synthesis advantages along with gelatin's own advantages. The insulin delivery from the framework after gelatin coating was ∼50%, which was ∼80% without coating at pH 3.5 and similar behavior at pH 7.2, suggesting that gelatin acts as an extra barrier for the insulin to get released. Thus, based on the release performance, good biocompatibility, hemocompatibility, and the presence of gelatin coating, we believe that **gel@insIITI-3** may be a potential candidate for an exciting possibility in the areas of protein and nucleic-acid-based oral delivery and can be extended for other diseases in the future.

ASSOCIATED CONTENT

Supporting Information

The Supporting Information is available free of charge at https://pubs.acs.org/doi/10.1021/acsmaterialslett.2c01175.

Experimental section including synthesis of H_4L linker and their characterizations (mass spectrometry, NMR spectroscopy), **IITI-3** (SC-XRD, PXRD, SEM, TGA, FT-IR, BET adsorption isotherm), cytotoxicity assay, and bright-field images; the activation of **IITI-3**, insulin encapsulation (**insIITI-3**), and modification with gelation (**gel@insIITI-3**), which are characterized by PXRD, SEM (EDX), TGA, FT-IR, BET adsorption isotherm, DLS, and zeta potential; comparison table (PDF)

AUTHOR INFORMATION

Corresponding Author

Shaikh M. Mobin − *Department of Chemistry, Indian Institute of Technology, Indore 453552, India; Department of Biosciences and Bio-Medical Engineering and Center for Electric Vehicle and Intelligent Transport Systems, Indian Institute of Technology Indore, Indore 453552, India;* orcid.org/0000-0003-1940-3822; Phone: +91-731-2438752; Email: xray@iiti.ac.in

Authors

Pawan Kumar − *Department of Chemistry, Indian Institute of Technology, Indore 453552, India*

Navpreet Kaur − *Department of Biosciences and Bio-Medical Engineering, Indian Institute of Technology Indore, Indore 453552, India*

Pranav Tiwari − *Department of Chemistry, Indian Institute of Technology, Indore 453552, India*

Anoop Kumar Gupta − *Department of Chemistry, Indian Institute of Technology, Indore 453552, India; Department of Chemistry, Pandit Prithi Nath College (C. S. J. M. University), Kanpur 208001 Uttar Pradesh, India*

Complete contact information is available at: https://pubs.acs.org/10.1021/acsmaterialslett.2c01175

Notes

The authors declare no competing financial interest.

■ ACKNOWLEDGMENTS

P.K. would like to thank Ministry of Education, Government of India for providing research fellowship. N.K. thanks UGC New Delhi for a fellowship. P.T. thanks BRNS (Project No. 58/14/17/2020-BRNS/37215). A.K.G. thanks IIT Indore for an Institute Postdoc fellowship. Additionally, A.K.G. sincerely acknowledges P. P. N. College Kanpur for research facilities and infrastructure. S.M.M. acknowledge SERB (CRG/2020/001769), BRNS (Project No. 58/14/17/2020-BRNS/37215) and IIT Indore for financial support. The authors gratefully acknowledge Dr. Ravinder, Mr. Kinny Pandey, Mr. Ghanshyam Bhavsar, and Mr. Nitin Upadhyay (Sophisticated Instrumentation Centre, IIT Indore) for characterization facilities. Authors are also thankful to Material Research Centre, MNIT Jaipur for providing the zeta potential facility. P.K. also thanks Dr. Viresh Kumar and Praveen Kumar for their help during manuscript preparation.

■ ABBREVIATIONS

DMF, dimethylformamide; MeOH, methanol; KOH, potassium hydroxide; CD, circular dichroism; DLS, dynamic light scattering; SI, Supporting Information

■ REFERENCES

(1) Moawd, S. A. Quality of Life in University Students with Diabetes Distress: Type 1 and Type 2 of Diabetes Differences. *J. Diabetes Res.* **2022**, *2022*, 1−7.
(2) Jiang, H.; Pang, S.; Zhang, Y.; Yu, T.; Liu, M.; Deng, H.; Li, L.; Feng, L.; Song, B.; Han-Zhang, H.; Ma, Q.; Qian, L.; Yang, W. A Phase 1b Randomised Controlled Trial of a Glucagon-like Peptide-1 and Glucagon Receptor Dual Agonist IBI362 (LY3305677) in Chinese Patients with Type 2 Diabetes. *Nat. Commun.* **2022**, *13*, 3613.
(3) Liu, R.; Liu, C.; He, X.; Sun, P.; Zhang, B.; Yang, H.; Shi, W.; Ruan, Q. MicroRNA-21 Promotes Pancreatic β Cell Function through Modulating Glucose Uptake. *Nat. Commun.* **2022**, *13*, 3545.
(4) Ukah, U. V.; Platt, R. W.; Auger, N.; Dasgupta, K.; Dayan, N. Development and Internal Validation of a Model to Predict Type 2 Diabetic Complications after Gestational Diabetes. *Sci. Rep.* **2022**, *12*, 10377.
(5) Rad, M. G.; Sharifi, M.; Meamar, R.; Soltani, N. The Role of Pancreas to Improve Hyperglycemia in STZ-Induced Diabetic Rats by Thiamine Disulfide. *Nutr. Diabetes* **2022**, *12*, 32.
(6) Volpatti, L. R.; Matranga, M. A.; Cortinas, A. B.; Delcassian, D.; Daniel, K. B.; Langer, R.; Anderson, D. G. Glucose-Responsive Nanoparticles for Rapid and Extended Self-Regulated Insulin Delivery. *ACS Nano* **2020**, *14*, 488−497.
(7) Zhao, Y.; Trewyn, B. G.; Slowing, I. I.; Lin, V. S.-Y. Mesoporous Silica Nanoparticle-Based Double Drug Delivery System for Glucose-Responsive Controlled Release of Insulin and Cyclic AMP. *J. Am. Chem. Soc.* **2009**, *131*, 8398−8400.
(8) Au, K. M.; Tisch, R.; Wang, A. Z. *In Vivo* Bioengineering of Beta Cells with Immune Checkpoint Ligand as a Treatment for Early-Onset Type 1 Diabetes Mellitus. *ACS Nano* **2021**, *15*, 19990−20002.
(9) Cho, N. H.; Shaw, J. E.; Karuranga, S.; Huang, Y.; da Rocha Fernandes, J. D.; Ohlrogge, A. W.; Malanda, B. IDF Diabetes Atlas: Global Estimates of Diabetes Prevalence for 2017 and Projections for 2045. *Diabetes Res. Clin. Pract.* **2018**, *138*, 271−281.
(10) Khan, M. A. B.; Hashim, M. J.; King, J. K.; Govender, R. D.; Mustafa, H.; al Kaabi, J. Epidemiology of Type 2 Diabetes − Global Burden of Disease and Forecasted Trends. *J. Epidemiol. Glob. Health* **2020**, *10*, 107.
(11) Kikkawa, R. Chronic Complications in Diabetes Mellitus. *Br. J. Nutr.* **2000**, *84*, 183−185.
(12) Porte, D., Jr. Clinical Importance of Insulin Secretion and Its Interaction with Insulin Resistance in the Treatment of Type 2 Diabetes Mellitus and Its Complications. *Diabetes Metab. Res. Rev.* **2001**, *17*, 181−188.
(13) Al-Tabakha, M.; Arida, A. Recent Challenges in Insulin Delivery Systems: A Review. *Indian J. Pharm. Sci.* **2008**, *70*, 278.
(14) Skyler, J. S.; Cefalu, W. T.; Kourides, I. A.; Landschulz, W. H.; Balagtas, C. C.; Cheng, S.-L.; Gelfand, R. A. Efficacy of Inhaled Human Insulin in Type 1 Diabetes Mellitus: A Randomised Proof-of-Concept Study. *Lancet* **2001**, *357*, 331−335.
(15) Benyettou, F.; Kaddour, N.; Prakasam, T.; Das, G.; Sharma, S. K.; Thomas, S. A.; Bekhti-Sari, F.; Whelan, J.; Alkhalifah, M. A.; Khair, M.; Traboulsi, H.; Pasricha, R.; Jagannathan, R.; Mokhtari-Soulimane, N.; Gándara, F.; Trabolsi, A. *In Vivo* Oral Insulin Delivery *via* Covalent Organic Frameworks. *Chem. Sci.* **2021**, *12*, 6037−6047.
(16) Chaturvedi, K.; Ganguly, K.; Nadagouda, M. N.; Aminabhavi, T. M. Polymeric Hydrogels for Oral Insulin Delivery. *J. Controlled Release* **2013**, *165*, 129−138.
(17) Chen, M.-C.; Sonaje, K.; Chen, K.-J.; Sung, H.-W. A Review of the Prospects for Polymeric Nanoparticle Platforms in Oral Insulin Delivery. *Biomaterials* **2011**, *32*, 9826−9838.
(18) Bai, Y.; Zhang, Z.; Zhang, A.; Chen, L.; He, C.; Zhuang, X.; Chen, X. Novel Thermo- and PH-Responsive Hydroxypropyl Cellulose- and Poly (l-Glutamic Acid)-Based Microgels for Oral Insulin Controlled Release. *Carbohydr. Polym.* **2012**, *89*, 1207−1214.
(19) Lopes, M.; Abrahim, B.; Seica, R.; Veiga, F.; Rodrigues, C.; Ribeiro, A. Intestinal Uptake of Insulin Nanoparticles: Facts or Myths? *Curr. Pharm. Biotechnol.* **2014**, *15*, 629−638.
(20) Huang, L.-L.; Yu, L.; Li, B.; Li, B.; Wang, H.; Li, J. Adsorption and Release of 1-Methylcyclopropene by Metal−Organic Frameworks for Fruit Preservation. *ACS Mater. Lett.* **2022**, *4*, 1053−1057.
(21) Zhou, Y.; Liu, L.; Cao, Y.; Yu, S.; He, C.; Chen, X. A Nanocomposite Vehicle Based on Metal−Organic Framework Nanoparticle Incorporated Biodegradable Microspheres for Enhanced Oral Insulin Delivery. *ACS Appl. Mater. Interfaces* **2020**, *12*, 22581−22592.
(22) Gupta, A. K.; Tomar, K.; Bharadwaj, P. K. Cd(ii) Coordination Polymers Constructed with a Flexible Carboxylate Linker and Pyridyl Co-Linkers: Variation in the Network Topologies and Photoluminescence Properties. *CrystEngComm* **2017**, *19*, 2253−2263.
(23) Horcajada, P.; Chalati, T.; Serre, C.; Gillet, B.; Sebrie, C.; Baati, T.; Eubank, J. F.; Heurtaux, D.; Clayette, P.; Kreuz, C.; Chang, J.-S.; Hwang, Y. K.; Marsaud, V.; Bories, P.-N.; Cynober, L.; Gil, S.; Férey, G.; Couvreur, P.; Gref, R. Porous Metal−Organic-Framework Nanoscale Carriers as a Potential Platform for Drug Delivery and Imaging. *Nat. Mater.* **2010**, *9*, 172−178.
(24) Rojas, S.; Colinet, I.; Cunha, D.; Hidalgo, T.; Salles, F.; Serre, C.; Guillou, N.; Horcajada, P. Toward Understanding Drug Incorporation and Delivery from Biocompatible Metal−Organic Frameworks in View of Cutaneous Administration. *ACS Omega* **2018**, *3*, 2994−3003.
(25) Férey, G. Hybrid Porous Solids: Past, Present, Future. *Chem. Soc. Rev.* **2008**, *37*, 191−214.
(26) Luo, W.; Bai, Z.; Zhu, Y. Fast Removal of Co(ii) from Aqueous Solution Using Porous Carboxymethyl Chitosan Beads and Its Adsorption Mechanism. *RSC Adv.* **2018**, *8*, 13370−13387.
(27) Prabaharan, M.; Mano, J. F. Chitosan-Based Particles as Controlled Drug Delivery Systems. *Drug Delivery* **2004**, *12*, 41−57.
(28) Peer, D.; Karp, J. M.; Hong, S.; Farokhzad, O. C.; Margalit, R.; Langer, R. Nanocarriers as an Emerging Platform for Cancer Therapy. *Nat. Nanotechnol.* **2007**, *2*, 751−760.
(29) Couvreur, P.; Gref, R.; Andrieux, K.; Malvy, C. Nanotechnologies for Drug Delivery: Application to Cancer and Autoimmune Diseases. *Prog. Solid State Chem.* **2006**, *34*, 231−235.
(30) Gref, R.; Minamitake, Y.; Peracchia, M. T.; Trubetskoy, V.; Torchilin, V.; Langer, R. Biodegradable Long-Circulating Polymeric Nanospheres. *Science (1979)* **1994**, *263* (263), 1600−1603.

https://doi.org/10.1021/acsmaterialslett.2c01175
ACS Materials Lett. 2023, 5, 1100−1108

(31) Chen, Y.; Li, P.; Modica, J. A.; Drout, R. J.; Farha, O. K. Acid-Resistant Mesoporous Metal−Organic Framework toward Oral Insulin Delivery: Protein Encapsulation, Protection, and Release. *J. Am. Chem. Soc.* **2018**, *140*, 5678−5681.
(32) Duan, Y.; Ye, F.; Huang, Y.; Qin, Y.; He, C.; Zhao, S. One-Pot Synthesis of a Metal−Organic Framework-Based Drug Carrier for Intelligent Glucose-Responsive Insulin Delivery. *Chem. Commun.* **2018**, *54*, 5377−5380.
(33) Suresh, K.; Matzger, A. J. Enhanced Drug Delivery by Dissolution of Amorphous Drug Encapsulated in a Water Unstable Metal−Organic Framework (MOF). *Angew. Chem., Int. Ed.* **2019**, *58*, 16790−16794.
(34) Wu, M.-X.; Yang, Y.-W. Metal-Organic Framework (MOF)-Based Drug/Cargo Delivery and Cancer Therapy. *Adv. Mater.* **2017**, *29*, 1606134.
(35) della Rocca, J.; Liu, D.; Lin, W. Nanoscale Metal−Organic Frameworks for Biomedical Imaging and Drug Delivery. *Acc. Chem. Res.* **2011**, *44*, 957−968.
(36) Nezhad-Mokhtari, P.; Arsalani, N.; Javanbakht, S.; Shaabani, A. Development of Gelatin Microsphere Encapsulated Cu-Based Metal-Organic Framework Nanohybrid for the Methotrexate Delivery. *J. Drug Delivery Sci. Technol.* **2019**, *50*, 174−180.
(37) Javanbakht, S.; Nezhad-Mokhtari, P.; Shaabani, A.; Arsalani, N.; Ghorbani, M. Incorporating Cu-Based Metal-Organic Framework/Drug Nanohybrids into Gelatin Microsphere for Ibuprofen Oral Delivery. *Mater. Sci. Eng.: C* **2019**, *96*, 302−309.
(38) Horcajada, P.; Serre, C.; Vallet-Regí, M.; Sebban, M.; Taulelle, F.; Férey, G. Metal−Organic Frameworks as Efficient Materials for Drug Delivery. *Angew. Chem., Int. Ed.* **2006**, *45*, 5974−5978.
(39) Nielsen, L.; Frokjaer, S.; Brange, J.; Uversky, V. N.; Fink, A. L. Probing the Mechanism of Insulin Fibril Formation with Insulin Mutants. *Biochemistry* **2001**, *40*, 8397−8409.
(40) Liu, K.; Zhang, J.-J.; Cheng, F.-F.; Zheng, T.-T.; Wang, C.; Zhu, J.-J. Green and Facile Synthesis of Highly Biocompatible Graphene Nanosheets and Its Application for Cellular Imaging and Drug Delivery. *J. Mater. Chem.* **2011**, *21*, 12034.
(41) Tiwari, P.; Kaur, N.; Sharma, V.; Mobin, S. M. High-Yield Graphene Produced from the Synergistic Effect of Inflated Temperature and Gelatin Offers High Stability and Cellular Compatibility. *Phys. Chem. Chem. Phys.* **2018**, *20*, 20096−20107.
(42) Kaur, N.; Sharma, V.; Tiwari, P.; Saini, A. K.; Mobin, S. M. Vigna Radiata" Based Green C-Dots: Photo-Triggered Theranostics, Fluorescent Sensor for Extracellular and Intracellular Iron(III) and Multicolor Live Cell Imaging Probe. *Sens. Actuators B Chem.* **2019**, *291*, 275−286.
(43) Bellido, E.; Hidalgo, T.; Lozano, M. V.; Guillevic, M.; Simón-Vázquez, R.; Santander-Ortega, M. J.; González-Fernández, A.; Serre, C.; Alonso, M. J.; Horcajada, P. Heparin-Engineered Mesoporous Iron Metal-Organic Framework Nanoparticles: Toward Stealth Drug Nanocarriers. *Adv. Healthc. Mater.* **2015**, *4*, 1246−1257.
(44) Zou, J.-J.; Wei, G.; Xiong, C.; Yu, Y.; Li, S.; Hu, L.; Ma, S.; Tian, J. Efficient Oral Insulin Delivery Enabled by Transferrin-Coated Acid-Resistant Metal-Organic Framework Nanoparticles. *Sci. Adv.* **2022**, *8* (8), abm4677.
(45) Souza, B. E.; Donà, L.; Titov, K.; Bruzzese, P.; Zeng, Z.; Zhang, Y.; Babal, A. S.; Möslein, A. F.; Frogley, M. D.; Wolna, M.; Cinque, G.; Civalleri, B.; Tan, J.-C. Elucidating the Drug Release from Metal−Organic Framework Nanocomposites via In Situ Synchrotron Microspectroscopy and Theoretical Modeling. *ACS Appl. Mater. Interfaces* **2020**, *12*, 5147−5156.
(46) Li, Z.; Peng, Y.; Xia, X.; Cao, Z.; Deng, Y.; Tang, B. Sr/PTA Metal Organic Framework as A Drug Delivery System for Osteoarthritis Treatment. *Sci. Rep.* **2019**, *9*, 17570.

https://doi.org/10.1021/acsmaterialslett.2c01175
ACS Materials Lett. 2023, 5, 1100−1108